Thermodynamic Regulation of Human Short-Chain Acyl–CoA Dehydrogenase by Substrate and Product Binding †

4 AUTHORS, INCLUDING:

Amy K Saenger
University of Minnesota Twin Cities
62 PUBLICATIONS **919** CITATIONS

Biochemical and Electrochemical Characterization of Two Variant Human Short-Chain Acyl-CoA Dehydrogenases[†]

Amy K. Saenger,[‡] Tien V. Nguyen,[§] Jerry Vockley,[§,⊥] and Marian T. Stankovich*,[‡]

Department of Chemistry, University of Minnesota, 207 Pleasant Street SE, Kolthoff and Smith Halls, Minneapolis, Minnesota 55455 and Department of Medical Genetics, Mayo Clinic and Foundation, Rochester, Minnesota 55905

Received June 2, 2005; Revised Manuscript Received September 15, 2005

ABSTRACT: Short-chain acyl-CoA dehydrogenase (hSCAD) catalyzes the first matrix step in the mitochondrial β-oxidation cycle with optimal activity toward butyryl- and hexanoyl-CoA. Two common variants of this enzyme encoding G185S and R147W substitutions have been identified at an increased frequency compared to the general population in patients with a wide variety of clinical problems, but functional studies of the purified mutant enzymes have shown only modestly changed kinetic properties. Moreover, both amino acid residues are located quite far from the catalytic pocket and the essential FAD cofactor. To clarify the potential relationship of these variants to clinical disease, we have further investigated their thermodynamic properties using spectroscopic and electrochemical techniques. Purified R147W hSCAD exhibited almost identical physical and redox properties to wild-type but only half of the specific activity and substrate activation shifts observed in wild-type enzyme. In contrast, the G185S mutant proved to have impairments of both its kinetic and electron transfer properties. Spectroelectrochemical studies reveal that G185S binding to the substrate/product couple produces an enzyme potential shift of only +88 mV, which is not enough to make the reaction thermodynamically favorable. For wild-type hSCAD, this barrier is overcome by a negative shift in the substrate/product couple midpoint potential, but in G185S this activation was not observed. When G185S was substrate bound, the midpoint potential of the enzyme actually shifted more negative. These results provide valuable insight into the mechanistic basis for dysfunction of the common variant hSCADs and demonstrate that mutations, regardless of their position in the protein structure, can have a large impact on the redox properties of the enzyme.

Human short-chain acyl-CoA dehydrogenase (hSCAD, E.C. 1.3.99.2)[1] is a mitochondrial enzyme that catalyzes the reversible two-electron oxidation as part of the mammalian β-oxidation cycle. Several members of the acyl-CoA dehydrogenase (ACD) family have been identified and their X-ray crystal structures have been solved, including both a bacterial and rat SCAD (*1*, *2*). SCAD is a homotetrameric enzyme consisting of four identical 44 kDa FAD-containing monomers, with maximal activity with butyryl-CoA as substrate.

* To whom correspondence should be addressed. Address: 207 Pleasant St. SE, Minneapolis, MN 55455. Phone: (612) 624-1019. Fax: (612) 626−7541. E-mail: stankovi@chem.umn.edu.

[‡] University of Minnesota.

[§] Mayo Clinic and Foundation.

[⊥] Present address: University of Pittsburgh School of Medicine, Children's Hospital of Pittsburgh, Department of Pediatrics, 3705 5th Avenue, Pittsburgh, PA 15213.

[1] Abbreviations: CoA, coenzyme A; FAD, flavin adenine dinucleotide; ACD, acyl-coenzyme A dehydrogenase; SCAD, short-chain acyl-coenzyme A dehydrogenase; ETF, electron-transferring flavoprotein; BCoA, butyryl-coenzyme A; CCoA, crotonyl-coenzyme A; E_m, general midpoint potential; $\hat{E}_m$, conditional midpoint potential; $E_{ox/hq}$, midpoint potential for the flavin oxidized/hydroquinone couple; $E_{ox/sq}$, midpoint potential for the flavin oxidized/semiquinone couple; $E_{BCoA/CCoA}$, midpoint potential for the butyryl-coenzyme A/crotonyl-coenzyme A couple; SHE, standard hydrogen electrode; SDS, sodium dodecyl sulfate; WT, wild-type.

Scheme 1: Acyl-CoA Oxidation Catalyzed by SCAD
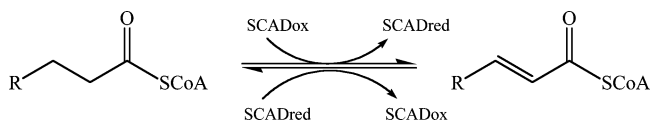
The formal reductive half-reaction catalyzed by hSCAD involves the abstraction of both a proton and a hydride ion from the α- and β-carbons of the thioester acyl-CoA substrate to yield the fully reduced ACD and enoyl-CoA (Scheme 1) (*3*, *4*). The two electrons transferred via this process are initially relocated to the flavin cofactor (FAD) after abstraction of the *pro-R* α-proton from the substrate by the catalytic base, Glu368, and the concerted *pro-R* β-hydride transfer to the N(5) of the FAD. The electrons then get shuttled to an electron-transferring flavoprotein (ETF) and are finally passed into the electron transport chain.

Previous redox studies in our laboratory have provided insight into the overall energetics of the ACD reaction and have revealed that substrate/product binding plays a critical role in the regulation of fatty acid metabolism. Uncomplexed hSCAD has a midpoint potential (E_m) of -162 mV (*5*), a value 122 mV more negative than that of the free substrate/product couple ($E_m = -40$ mV). Upon binding of the natural substrate/product couple (butyryl/crotonyl-CoA), the E_m of the flavin shifts positive 110 mV, thus becoming nearly isopotential with the free substrate/product couple. The small thermodynamic barrier remaining (12 mV) is overcome by

a large negative shift in the potential of the actual substrate/product couple itself (33 mV). Potential shifts such as those seen in hSCAD have also been observed in bacterial SCAD (bSCAD) and mammalian medium-chain acyl-CoA dehydrogenase (MCAD) (*6, 7*). However, the large degree of substrate activation observed in hSCAD is significant in that both the enzyme *and* the substrate itself require modulation for the previously unfavorable reaction to become favorable and proceed in an efficient manner, a feat not necessary in the other enzymes.

Inborn errors of the ACDs are significant causes of morbidity and mortality in humans. SCAD deficiency has been reported with extremely heterogeneous presentations, making it difficult to diagnose on a clinical basis. Abnormal accumulation of ethylmalonic acid (EMA) in the urine is the hallmark sign of SCAD deficiency and presumably reflects an intracellular accumulation of butyryl-CoA (*8, 9*). Two polymorphisms, G625A and C511T, have been described in the SCAD gene and are more commonly found in patients with elevated urine EMA and a variety of neurologic conditions than in the general population (*9, 10*). These variant alleles result in glycine/serine and arginine/tryptophan amino acid substitutions at positions 185 (G185S) and 147 (R147W) in the mature SCAD enzyme, leading to mild impairment of enzymatic function and increased thermolability compared to wild-type SCAD. Near UV−CD spectroscopy indicates that decreased stability in these mutants is caused by decreased flexibility in the tertiary conformation, and in vitro studies have demonstrated impaired folding of the variant proteins after import into mitochondria; however, the physiologic relevance of these abnormalities remains unclear (*10, 11*).

Both thermodynamic and kinetic characteristics are important in determining the mechanistic properties of enzymes. In the present study, the biophysical, enzymatic, and thermodynamic properties of the two mutant hSCAD enzymes were investigated using spectroelectrochemical techniques complemented by kinetic studies to evaluate the ability of the two mutant enzymes to accomplish electron transfer. By investigating redox modulation of the two SCAD enzymes, we seek to provide additional insight into the molecular basis for SCAD deficiency in humans.

MATERIALS AND METHODS

Protein Expression and Purification. Recombinant wild-type hSCAD was purified as described previously (*5*). hSCAD and other ACDs produced in bacterial expression systems typically exhibit a bright green color due to a CoA persulfide bound to the enzyme (*12*). To remove the CoASH, a thiopropyl-Sepharose 6B (Pharmacia; Piscataway, NJ) column was used. The A280/450 ratio of the enzyme was 4.5, indicating sufficient binding of the flavin. The final peak fractions were pooled and dialyzed against 50 mM potassium phosphate (KP$_i$) buffer (pH 7.6) for storage at −80 °C with glycerol until use. Concentration of the protein was calculated using the extinction coefficient determined for hSCAD (14.5 ± 0.2 mM^{-1} cm^{-1}) using the method of Williamson and Engle (*12*).

Polymerase chain reaction (PCR) site-directed mutagenesis was used to construct the mutant SCAD cDNA sequences from the cloned wild-type hSCAD gene as described (*10*).

Mutagenic primers were synthesized by the Molecular Biology Core Facility at the Mayo Clinic (Rochester, MN). For the C511T variation, the upstream PCR primer was 5′-CGT GCC ACC ACC GCC **TGG** GCC GAG GGC G-3′, and for the G625A variation it was 5′-GAC AGA GCC CTG CAA AAC AAG **AGC** ATC AGT GCC TTC CTG GTC-3′. The underlined bold nucleotides indicate those nucleotides that differ from wild-type hSCAD. PCR products were digested with *Apa*I (Boehringer Mannheim; Mannheim, Germany) and *Bgl*II (Gibco BRL) and inserted into the pKK223-3 (Pharmacia; Uppsala, Sweden) expression vector. All hSCAD plasmids and a plasmid containing the genes for the bacterial chaperonins GroEL and GroES were introduced into the *E. coli* host strain XL1 Blue (Stratagene; La Jolla, CA) and maintained under selective conditions appropriate for each plasmid (*10*).

Expression of the mutant hSCAD proteins was essentially performed as described above and by Nguyen et al. (*10*) with minor modifications. This included growth in Terrific broth, harvesting cells 4 h after induction with isopropylthio-β-D-galactoside (IPTG), disruption by sonication, and removal of cellular debris through centrifugation. Mutant hSCAD was purified from the crude cellular extract by chromatography on a DEAE-Sepharose column, fractionation with 45−65% ammonium sulfate, and through use of a 20 μM ceramic hydroxyapatite FPLC column.

Sodium dodecyl sulfate−polyacrylimide gel electrophoresis (SDS−PAGE) was used to determine the purity of all enzymes. All experiments utilized enzyme of greater than 95% purity at 25 °C. Activity assays were performed using ferricenium as the terminal electron acceptor (*13*). Molar extinction coefficients of the oxidized wild-type and hSCAD mutants were determined by the guandinium hydrochloride method of Williamson and Engel (*12*). Purified protein was stored in 50 mM potassium phosphate buffer (pH 7.6) at −80 °C with 20% glycerol prior to use.

Materials. Butyryl-CoA and crotonyl-CoA were purchased from Sigma Chemical Company (St. Louis, MO). The following dyes were used in electrochemical experiments: methyl viologen (Sigma), indigo disulfonate (Aldrich), pyocyanine (photochemically synthesized from phenazine methosulfate (Sigma)), and 8-chlororiboflavin (a generous gift from Dr. J. P. Lambooy, University of Maryland). All experiments utilized glass-distilled water.

Anaerobic Titrations of Wild-Type and Mutant SCAD with Substrate. G185S and R147W hSCAD were titrated with butyryl-CoA substrate as described in detail previously (*5*). The titration was accomplished by degassing a mixture containing 12−15 μM of the hSCAD enzyme, 100 μM methyl viologen, and buffer (50 mM KP$_i$, pH 7.6) in the cuvette of the spectroelectrochemical cell. The system was then electrochemically reduced to remove any residual oxygen. Aliquots of anaerobic 1.5 mM butyryl-CoA were added via a gastight syringe (Hamilton Company; Reno, NV) through a port in the cell. After each addition of substrate, spectral changes occurred within the system after a maximum time of 10 min, at which point the visible spectrum was obtained. Spectral scans were performed using a Perkin-Elmer Lambda 12 spectrophotometer equipped with an IBM-compatible computer.

Binding Constants. The dissociation constants (K_{dox}) for the G185S hSCAD enzyme complexed with butyryl-CoA

or crotonyl-CoA were determined by aerobic titration of the enzyme (ca. 50 μM) with a known amount of ligand at 25 °C. Small amounts of ligand were added to the enzyme solution in a reduced volume quartz cuvette via a modified syringe. Absorbance perturbations in the flavin spectrum occur due to desolvation of the active site (*14*), and these changes are monitored throughout the experiment at approximately 485 nm. Nonlinear regression analyses of binding titrations were performed using GraphPad Prizm version 3.00 for Windows (GraphPad Software; San Diego, CA).

Spectroelectrochemical Methods. Potentiometric and coulometric experiments were performed in a spectroelectrochemical cell at 25 °C in 50 mM potassium phosphate buffer (pH 7.6) as previously described (*6, 15*). Visible spectra were recorded with a Perkin-Elmer Lambda 12 UV−Vis spectrophotometer equipped with a thermostated cell and a stirring mechanism. In coulometric titrations, a 10−15 μM enzyme solution was used, along with methyl viologen (100 μM) as the mediator dye. Potentiometric experiments utilized the same solution composition as coulometric experiments, with the addition of three indicator dyes (2−5 μM): indigo disulfonate ($E_m = -118$ mV, pH 7.6), pyocyanine ($E_m = -19$ mV, pH 7.6), and 8-chlororiboflavin ($E_m = -162$ mV, pH 7.6). Equilibration between the solution and the gold working electrode typically took 1−2 h per point and was defined by a change in potential of <1 mV/10 min. All potential measurements are reported versus the standard hydrogen electrode (SHE).

To determine the midpoint potential of the hSCAD mutants in the presence of the natural substrate/product couple (butyryl-CoA/crotonyl-CoA), we performed experiments essentially as previously described by Stankovich and Soltysik (*6*). The spectroelectrochemical glass cuvette contained approximately 15 μM enzyme, 100 μM methyl viologen, 2 μM indigo disulfonate, and 5 μM pyocyanine in 50 mM potassium phosphate buffer (pH 7.6). In the sidearm of the cell resided the substrate/product couple solution. Once the contents of the cell were degassed, the system was electrochemically reduced to a point near the expected equilibrium. Reduction was performed to remove any residual oxygen and to require less turnover of substrate and product to achieve equilibrium. The substrate/product couple solution was then tipped into the cell and the final concentration of the couple was approximately 150 μM, with a final protein concentration of approximately 10−12 μM. A 10-fold excess of substrate and product ensured that the measured potential was that of the system, equilibrating near the potential of the free, unbound couple (−40 mV) (*7*). Equilibrium of the system was attained when the change in measured potential was less than 1 mV/30 min. This typically took less than 1.5 h, at which point the potential of the system was recorded and the visible spectra was obtained.

Coulometric and Potentiometric Titration Calculations. Prior to quantitation, spectra were corrected for dyes by subtracting the spectra of each dye at the measured potential. If necessary the spectra were also corrected for turbidity. The number of reducing equivalents, n, was calculated in coulometric titrations based on the number of moles of enzyme present in the sample and potentiometric data was calculated using the Nernst equation.

Table 1: Spectral Properties[a] of Oxidized Wild-Type and Mutant hSCAD and Substrate and Product Complexed G185S hSCAD

enzyme	ligand	λ_{max} (nm)	ϵ_λ (mM^{-1} cm^{-1})
wild-type	none	448	14.5 ± 0.2
R147W	none	446	14.3 ± 0.4
G185S	none	449	14.2 ± 0.3
	butyryl-CoA	449	14.2 ± 0.1
	crotonyl-CoA	452	14.0 ± 0.3

[a] Maximum wavelength (λ_{max}) and extinction coefficient (ϵ_λ).
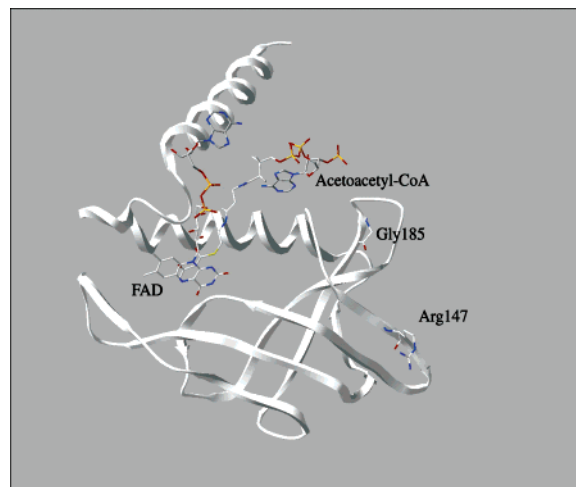

FIGURE 1: Schematic representation of the SCAD monomer based on the crystal structure (Protein Data Bank code 1JQI).

RESULTS AND DISCUSSION

Expression and Purification of Mutant hSCAD Proteins. All wild-type and mutant enzyme solutions exhibited a bright yellow or green color, indicative of the oxidized holoprotein. The enzymes were purified to homogeneity and showed distinct 44 kDa SDS−polyacrylamide gel bands similar to those seen in the wild-type enzyme (data not shown). The λ_{max} values and the extinction coefficients calculated for each enzyme are presented in Table 1. The G185S and R147W spectra showed characteristic flavin bands and are similar to the WT hSCAD spectrum. The absorbance spectra of the mutant enzymes shows only small changes compared to WT hSCAD. This is not surprising given that these mutations are located quite far (ca. 18 Å) from the FAD cofactor (Figure 1) (*2*) and likely minimally affect the structure of active site. Both purified mutant hSCAD enzymes were green in color, indicative of the presence of a bound CoA persulfide. Removal of the CoASH slightly affected the stability of the enzyme; thus, CoASH abstraction was performed immediately prior to all experiments. Bound CoA persulfide has previously been shown not to greatly affect the kinetic properties of the purified enzymes (*10*); however, it does alter behavior in electrochemical experiments (*11*).

The activity of wild-type, R147W, G185S, and hSCAD with butyryl-CoA was measured with ferricenium as electron acceptor (*13*), and kinetic parameters for each enzyme are presented in Table 2. The same parameters previously measured with the physiologic enzyme acceptor electron transferring flavoprotein (ETF) were modestly impaired for the G185S mutant (the specific activity and tetramer catalytic efficiency were approximately one-half and one-third, respectively, of values obtained with the wild-type enzyme).

Table 2: Kinetic Parameters[a] of Wild-Type and Variant SCAD Measured Using the Ferricenium Assay Utilizing Butyryl-CoA as the Substrate

enzyme	K_m (μM)	V_{max} (s^{-1})[b]	V_{max}/K_m (mM s^{-1})
wild-type	55 ± 8	34 ± 2	618 ± 25
R147W	65 ± 6	23 ± 5.7	354 ± 33
G185S	124 ± 12	3.8 ± 0.8	31 ± 18

[a] Determined at 25 °C in 50 mM potassium phosphate buffer (pH 7.6) using 200 μM ferricenium. [b] V_{max} expressed in [FcPF$_6$]•[FAD]$^{-1}$s^{-1}.

Table 3: Midpoint Potentials[a] for Wild-Type and Mutant hSCAD

enzyme	$E_{ox/hq}$ (mV)[b]	$\Delta E_{ox/hq}$ (mV)	% Sq[c]	$\hat{E}_{ox/hq}$ (mV)[b,d]
wild-type	-162[e]	0	<5.0	-52[e]
R147W	-163	-1	<5.0	-54
G185S	-150	$+12$	<5.0	-62
G185S/BCoA	-174	-24[f]	<5.0	
G185S/CCoA	-65	$+85$[f]	<5.0	

[a] Potentials reported in mV at 25 °C in 50 mM potassium phosphate buffer (pH 7.6). [b] All midpoint potential determinations were calculated from an average of three trials with a typical error of $\pm$ 2−5 mV. [c] Maximum percentage of blue neutral semiquinone stabilized during potentiometric titrations of oxidized enzyme. [d] Conditional midpoint potential measured with BCoA/CCoA. [e] From ref 5. [f] $\Delta E_{ox/hq}$ calculated as difference in potential between uncomplexed and ligand complexed G185S hSCAD.

Values obtained for the R147W mutant were comparable to wild-type enzyme (*10*). Similar results were obtained using the ferricenium assay. The K_m of the G185S mutant was the highest, and the V_{max}/K_m the lowest of the three enzymes, which indicated that is the most catalytically inefficient. Although the V_{max}/K_m of the R147W enzyme is only half of that determined for WT hSCAD, the variant is still a relatively efficient and thus functional enzyme.

Spectroelectrochemical Measurements of Free G185S and R147W hSCAD. Wild-type hSCAD is a highly thermodynamically modulated enzyme with a free midpoint potential of −162 mV, the most negative of any acyl-CoA dehydrogenase electrochemically studied in our laboratory. The electron transfer properties of the uncomplexed hSCAD variant enzymes were investigated to characterize the effect of these mutations on the redox properties of the enzymes. Coulometric titrations of the two enzymes were performed initially to ensure that a two-electron reduction was occurring, and indeed both R147W and G185S had a calculated value of $n \approx 2.2$. No major spectral differences were observed between coulometric reduction of the wild-type and mutant hSCADs and less than 5% of either blue or red semiquinone was stabilized throughout the course of the titrations.

The two-electron reduction potentials ($E_{ox/hq}$) of the enzymes were then established through potentiometric titrations. A typical potentiometric titration is presented in Figure

2 and the calculated enzyme reduction potentials are shown in Table 3. The $E_{ox/hq}$ for wild-type hSCAD (−162 mV) is only slightly more negative than the $E_{ox/hq}$ potential determined for the G185S mutant (−150 mV) and essentially identical to the $E_{ox/hq}$ for R147W (−163 mV). It was expected that both the Gly → Ser and Arg → Trp mutations would have only slight effects on the enzyme redox potential due to their position in the enzyme monomer >18 Å distance from the FAD cofactor. Further structural implications of these mutations will be discussed further in subsequent sections. Less than 5% of semiquinone was stabilized in the protein titrations; thus, the formal potential values cannot be accurately calculated.

$\hat{E}_{ox/hq}$ *of hSCAD Mutants in the Presence of BCoA and CCoA.* Binding of the substrate/product couple has been shown to be essential for enzymatic function in acyl-CoA dehydrogenases (*6, 7*). Thermodynamic information regarding the effects of binding on the enzyme potential is obtained through measurement of the enzyme reduction potential upon addition of an excess of the substrate/product couple. The calculated enzyme potential when substrate/product bound
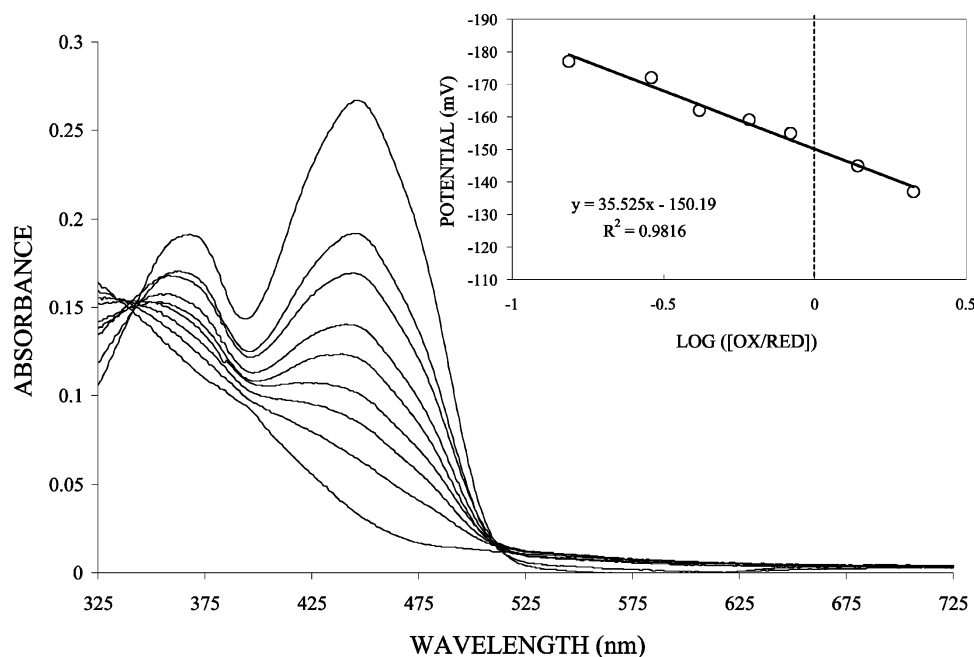

FIGURE 2: Potentiometric titration of uncomplexed G185S hSCAD. Titration was performed in 50 mM potassium phosphate buffer (pH 7.6) at 25 °C under anaerobic conditions. Solution contained 100 μM methyl viologen, 2 μM indigo disulfonate, 5 μM pyocyanine, and 2 μM 8-chlororiboflavin. Curve 1, fully oxidized spectrum. Curves 2−8, E = −137, −145, −155, −159, −162, −172, and −177 mV, respectively. Curve 9, fully reduced spectrum. Inset: Nernst plot indicating E_m = −150 mV.
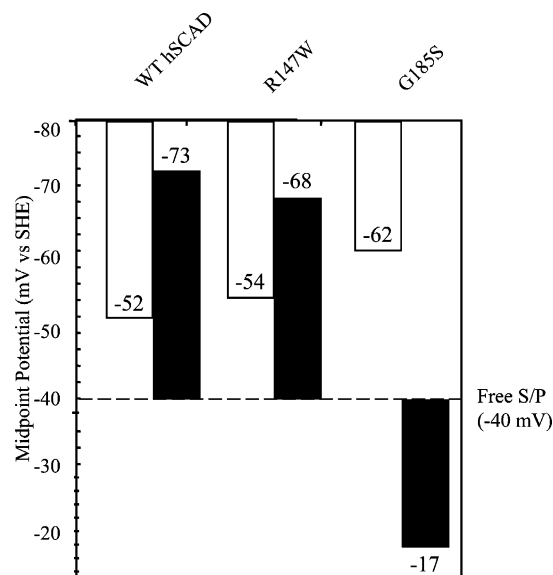
FIGURE 3: Comparison of the BCoA/CCoA couple potential shifts and flavin midpoint potential shifts in the WT and variant hSCAD•substrate/product complexes. The unfilled bars represent the enzyme potential shift when bound to each specific S/P couple ($\hat{E}_{ox/hq}$). The solid bars signify the midpoint potential shift of the S/P couple upon binding to hSCAD. The dotted line indicates the midpoint potential of the free BCoA/CCoA couple (−40 mV).

is referred to as the conditional midpoint potential ($\hat{E}_{ox/hq}$). It has previously been shown that wild-type hSCAD exhibits a large potential shift (110 mV) upon substrate/product binding (5). Thus, the act of binding itself is considered to be responsible for a large portion of the thermodynamic modulation observed in wild-type hSCAD.

To examine these same binding effects in the recombinant variant hSCAD mutants, we determined the conditional midpoint potentials ($\hat{E}_{ox/hq}$) of the mutant enzymes in the presence of their optimal substrate couple, butyryl-CoA and crotonyl-CoA as previously described (6, 16). Spectral changes that occurred upon addition of the 1:1 BCoA/CCoA couple were typical of those seen in these types of experiments. To calculate the concentration of oxidized and reduced mutant hSCAD present at equilibrium, the free oxidized molar absorptivities were as presented in Table 1, and CCoA-bound R147W and G185S molar absorptivities were calculated as 13.6 ± 0.5 and 14.0 ± 0.3 mM^{-1} cm^{-1}. The $\hat{E}_{ox/hq}$ values for the G185S and R147W proteins were experimentally determined to be −62 and −54 mV, respectively (Table 3, pictorially shown in Figure 3, unfilled bars).

The $\hat{E}_{ox/hq}$ for R147W hSCAD is extremely similar to that of wild-type hSCAD, suggesting that this mutation is of no apparent consequence in determining the redox properties of the flavin. The $\hat{E}_{ox/hq}$ value calculated for G185S (−62 mV) was 10 mV more negative than that of the wild-type protein; thus, binding of the substrate/product couple does not produce as large of a shift in the FAD cofactor. Comparison of the $E_{ox/hq}$ and $\hat{E}_{ox/hq}$ values for each protein shows that electron transfer to the acyl-CoA thioester (−40 mV) is still unfavorable for each enzyme at this point. Therefore, to determine the extent of modulation in each of these enzymes the contributions from the substrate/product themselves also need to be considered.

Anaerobic Titrations of hSCAD Mutants with Butyryl-CoA. The actual potential of the substrate/product couple cannot

be measured during electrochemical experiments due to the overlapping spectra of the thioester and the protein in the UV region. To determine the contributions of the thioester couple to enzyme modulation, anaerobic substrate titrations were performed with each variant enzyme, and a conditional potential difference ($\Delta\hat{E}$) was calculated. $\Delta\hat{E}$ is defined as the difference between the $\hat{E}_{ox/hq}$ value and the $E_{sub/prod}$ couple (6, 7). Titration of wild-type hSCAD with BCoA resulted in a $\Delta\hat{E}$ value of −21 mV, with the potential for the enzyme being more positive. This large shift in the BCoA/CCoA couple in the hSCAD system allows for electron transfer to proceed and represents the greatest substrate activation of any ACD studied. While both hSCAD mutants also demonstrate some degree of modulation, an energy barrier still remains for electron transfer to commence. Substrate titrations of the two mutants yield additional information about how the potential of the substrate/product couple changes upon binding to the enzyme.

Figure 4 shows the progression of the titration of G185S and R147W hSCAD with butyryl-CoA. The spectra from the two experiments are starkly different in that very little reduction is seen in the G185S mutant. This is in contrast to the results obtained with anaerobic substrate titrations with wild-type or R147W enzyme. Interaction of an acyl-CoA dehydrogenase with a substrate is typically studied by monitoring the characteristic absorbance changes at 450 and 580 nm following the addition of substrate to enzyme under anaerobic conditions. A decrease in the absorbance at 450 nm is characteristic of the reduction of the essential flavin cofactor, while an increase in absorbance at 580 nm is due to a new resonance signal related to formation of the stable charge-transfer complex in the enzyme reaction (17−19). However, in the G185S hSCAD mutant the flavin band does not decrease, and no charge-transfer band is observed. Even after excessive amounts of butyryl-CoA are added (10−50-fold excess) to the solution, only very small amounts of reduced enzyme are observed (2.9% bleaching). This suggests that the stable charge-transfer intermediate seen when either wild-type or R147W hSCAD is titrated with butyryl-CoA does not form with the G185S mutant. These results, coupled with the impaired kinetic properties observed in this mutant, suggest that the G185S enzyme does not properly utilize its optimum substrate.

As noted, only 2.9% reduction with excess substrate was observed for the G185S enzyme as compared to the considerably higher bleaching obtained with the wild-type (83%) and R147W (72%) enzymes. These $\Delta\hat{E}$ values are calculated from the spectra acquired during the substrate titrations and correspond to values of +45, −14, and −21 mV for G185S, R147W, and wild-type hSCAD, respectively (Figure 3, solid bars). This indicates that product formation actually appears to be made *more* difficult by binding of substrate to the G185S mutant. It would appear that the substrate binding cavity in G185S enzyme does not allow for favorable formation of the charge-transfer complex after binding of substrate. Because the G185S mutant lies at the beginning of a β-strand at the opening of the substrate binding pocket (Figure 1) it is likely that the Gly → Ser mutation induces a conformational change in the enzyme that does not allow the thermodynamic modulation observed in other ACD systems to occur. On the other hand, the R147W mutation is exposed to solvent on a different β-strand
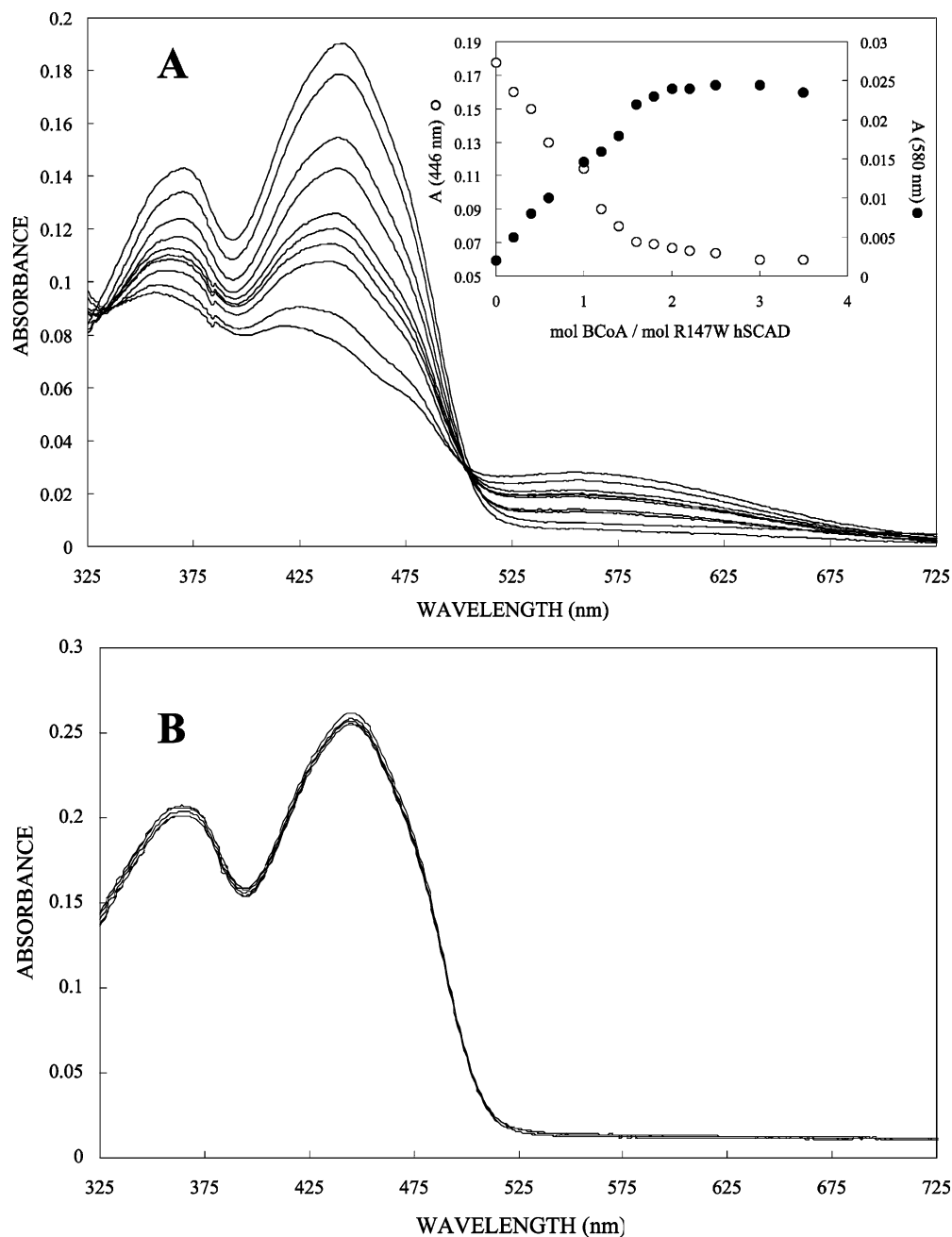
FIGURE 4: Reductive titration of R147W and G185S hSCAD with butyryl-CoA substrate. Titrations were performed in 50 mM potassium phosphate buffer, pH 7.6 under anaerobic conditions at 25 °C. Solutions contained 100 μM methyl viologen and spectra have been subtracted for turbidity. (A) Titration of R147W hSCAD (13.6 μM) with butyryl-CoA. Only selected spectra are shown for clarity. Inset: Plot of absorbance at 446 nm (○) and 580 nm (●) as a function of substrate added. (B) Titration of G185S hSCAD (16.1 μM) with butyryl-CoA. Only selected spectra are shown for clarity.

that does not appear to participate significantly in interactions with substrate (*2*). These results are consistent with the previous hypothesis predicting an electron-transfer impediment in the G185S hSCAD protein.

Binding and Electrochemical Characterization of BCoA and CCoA Bound G185S. Diminished reduction of the G185S enzyme with BCoA as demonstrated with anaerobic substrate titrations is indicative of a lack of electron transfer from the thioester couple to the FAD cofactor. The overall activity of the G185S variant under anaerobic conditions was also less than 5% of the activity of wild-type hSCAD as measured with BCoA. Thus, the G185S variant can be treated essentially as a kinetically impaired enzyme and this allows for examination of the binding and electrochemical properties

of BCoA-bound and CCoA-bound G185S to be examined separately as for the catalytic base mutant E368Q (*5*).

The overall appearance of both BCoA and CCoA bound G185S complexes are similar to those seen in similar studies with the kinetically dead E368Q hSCAD mutant bound to natural thioester ligands, with a slight red shift of the flavin upon binding and growth of a shoulder at ca. 485 nm (data not shown). The dissociation constants (K_{dox}) calculated for BCoA and CCoA bound G185S are 10.3 μM and 246 nM, respectively. Clearly binding of each ligand is not greatly affected by the G185S mutation, although the product binds 40 times more tightly than substrate. This is reasonable based on the known structure of the wild-type human enzyme where neither the G185 nor the R147 residues appear to be

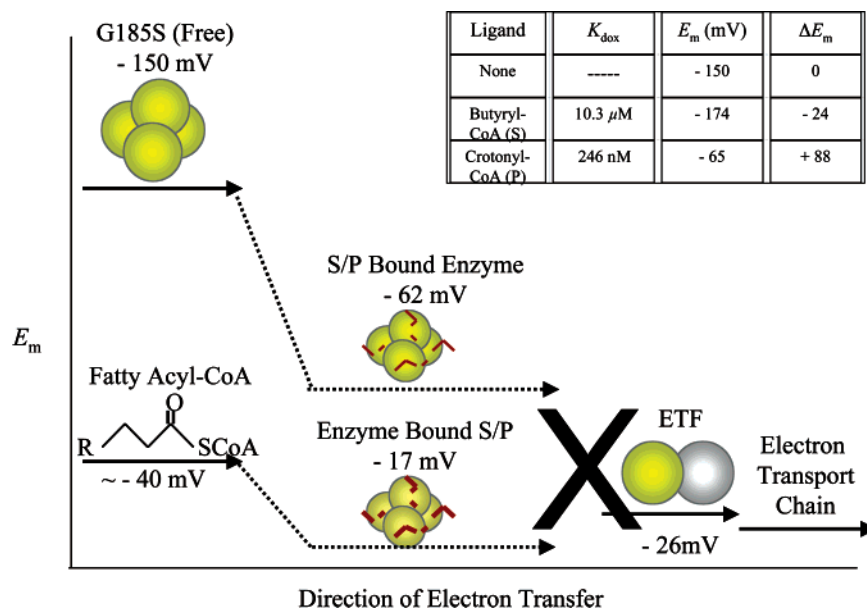| Ligand	K_{dox}	E_m (mV)	ΔE_m
None	-----	- 150	0
Butyryl-CoA (S)	10.3 μM	- 174	- 24
Crotonyl-CoA (P)	246 nM	- 65	+ 88

FIGURE 5: Overall thermodynamic modulations induced by enzyme/ligand binding in G185S hSCAD. Potential for S/P bound enzyme measured using excess substrate/product couple. Potential for enzyme bound S/P determined through calculation of $\Delta \hat{E}$.

directly involved with the tetramer interface, substrate binding, flavin binding, or catalysis (*2*). Rather, it is more probable that the mutations at these positions induce secondary changes that in turn decrease the geometry of the catalytic site and thus impair catalysis.

Coulometric titrations were initially performed using substrate or product saturated G185S enzyme solutions to ensure that the reaction required two electrons and no co-reduction was taking place. This was in fact seen and thus allowed measurement of the midpoint potential. The calculated $E_{ox/hq}$ values for BCoA or CCoA saturated G185S solutions are shown in Table 3. When the enzyme is substrate bound the midpoint potential actually shifts negative 24 mV, a result that was surprising but consistent with the earlier electrochemical data. Thus, binding of BCoA makes enzyme modulation *less* favorable, reinforcing our previous observation of the lack of electron transfer from substrate to the flavin. The $E_{ox/hq}$ value for CCoA bound G185S is −65 mV, a value similar to that obtained when the enzyme was bound to BCoA/CCoA (−62 mV). We postulate that product binding is responsible for the large potential changes observed since substrate binding appears to inhibit electron transfer. A graphical representation of our model for thermodynamic modulation involved in the activation of the G185S/BCoA complex is shown in Figure 5. As demonstrated, the potential of the G185S bound to the substrate/product couple is significantly shifted in the positive direction. However, when BCoA is bound, the midpoint potential of the enzyme is only slightly altered and the actual substrate/product couple does not produce the thermodynamic destabilization necessary to create a potential overlap similar to that seen with wild-type and R147W hSCAD. This is the first direct evidence of a human mutation exhibiting electron-transfer difficulties.

CONCLUSION

These data provide insight into the thermodynamic properties of two recently discovered polymorphic hSCAD variants, G185S and R147W. We conclude that the G185S hSCAD

enzyme appears incapable of electron transfer from the substrate to the FAD cofactor at the appropriate levels needed for catalysis to proceed. The R147W variant, however, exhibits similar redox properties to wild-type enzyme, and if it contributes to metabolic diseases, it is likely through a noncatalytic means. In this regard, it has been shown that both mutations affect folding in a temperature-sensitive manner (*20*, *21*).

Examination of the crystal structure of rat SCAD leads to ready potential explanations of our findings. R147 is located on a β-barrel motif that does not directly contribute to monomer interactions or binding of FAD in the substrate binding pocket (*2*). In contrast, G185 is predicted to be located near the opening of the substrate binding pocket. Therefore, while it is not likely to directly interact with the substrate, substitution of the glycine residue with a serine alters the hydrophobicity of the local protein environment and likely alters the redox properties. Binding of FAD to enzyme is not predicted to be affected by mutation, and our binding studies confirm this in the G185S variant. Overall, our thermodynamic, kinetic, and spectroscopic data provide a better understanding of the function of the common variant SCAD enzymes and their potential contribution to clinical disease in humans.

REFERENCES

1. Djordjevic, S., Pace, C. P., Stankovich, M. T., and Kim, J.-J. (1995) Three-dimensional structure of butyryl-CoA dehydrogenase from Megasphaera elsdenii, *Biochemistry 34*, 2163−2171.
2. Battaile, K., Molin-Case, J., Paschke, R., Wang, M., Bennett, D. W., Vockley, J., and Kim, J.-J. (2002) Crystal structure of rat short chain acyl-CoA dehydrogenase complexed with acetoacetyl-CoA: comparison with other acyl-CoA dehydrogenases, *J. Biol. Chem. 277*, 12200−12207.

3. Ghisla, S., Thorpe, C., and Massey, V. (1984) Mechanistic studies with general acyl-CoA dehydrogenase and butyryl-CoA dehydrogenase: evidence for the transfer of the beta-hydrogen to the flavin N(5)-position as a hydride, *Biochemistry 23*, 3154−3161.

4. Frerman, F. E., Kim, J. J., Huhta, K., and McKean, M. C. (1980) Properties of the general acyl-CoA dehydrogenase from pig liver, *J. Biol. Chem. 255*, 2199−2202.

5. Saenger, A. K., Nguyen, T., Vockley, J., and Stankovich, M. T. (2005) *Biochemistry*, *44*, 16043−16053.

6. Stankovich, M. T., and Soltysik, S. (1987) Regulation of the butyryl-CoA dehydrogenase by substrate and product binding, *Biochemistry 26*, 2627−2632.

7. Lenn, N. D., Stankovich, M. T., and Liu, H. (1990) *Biochemistry 29*, 3709−3715.

8. Corydon, M. J., Gregersen, N., Lehnert, W., Ribes, A., Rinaldo, P., Kmoch, S., Christensen, E., Kristensen, T. J., Andresen, B. S., Bross, P., Winter, V., Martinez, G., Neve, S., Jensen, T. G., Bolund, L., and Kolvraa, S. (1996) Ethylmalonic aciduria is associated with an amino acid variant of short chain acyl-coenzyme A dehydrogenase, *Pediatr. Res. 39*, 1059−1066.

9. Gregersen, N., Winter, V., Corydon, M. J., Corydon, T. J., Rinaldo, P., Ribes, A., Martinez, G., Bennett, M. J., Vianey-Saban, C., Bhala, A., Hale, D. E., Lehnert, W., Kmoch, S., Roig, M., Riudor, E., Eiberg, H., Anderson, B., Bross, P., Bolund, L. A., and Kolvraa, S. (1998) Identification of four new mutations in the short-chain acyl-CoA dehydrogenase (SCAD) gene in two patients: one of the variant alleles, 511C → T, is present at an unexpectedly high frequency in the general population, as was the case for 625G → A, together conferring susceptibility to ethylmalonic aciduria, *Hum. Mol. Genet. 7*, 619−627.

10. Nguyen, T. V., Riggs, C., Babovic-Vuksanovic, D., Kim, Y.-S., Carpenter, J. F., Burghardt, T. P., Gregersen, N., and Vockley, J. (2002) Purification and characterization of two polymorphic variants of short chain acyl-CoA dehydrogenase reveal reduction of catalytic activity and stability of the Gly185Ser enzyme, *Biochemistry 41*, 11126−11133.

11. Pederson, C. B., Bross, P., Winter, V. S., Corydon, T. J., Bolund, L., Bartlett, K., Vockley, J., and Gregersen, N. (2003) Misfolding, degradation, and aggregation of variant proteins. The molecular pathogenesis of short chain acyl-CoA dehydrogenase (SCAD) deficiency, *J. Biol. Chem. 278*, 47449−47458.

12. Williamson, G., and Engel, P. C. (1982) A convenient and rapid method for the complete removal of CoA from butyryl-CoA dehydrogenase, *Biochim. Biophys. Acta 706*, 245−248.

13. Lehman, T. C., Hale, D. E., Bhala, A., and Thorpe, C. (1990) An acyl-coenzyme A dehydrogenase assay utilizing the ferricenium ion, *Biochemistry 186*, 280−284.

14. Trievel, R. C., Wang, R., Anderson, V. E., and Thorpe, C. (1995) Role of the carbonyl group in thioester chain length recognition by the medium chain acyl-CoA dehydrogenase, *Biochemistry 34*, 8597−8605.

15. Stankovich, M. T. (1980) An anaerobic spectroelectrochemical cell for studying the spectral and redox properties of flavoproteins, *Anal. Biochem. 109*, 295−308.

16. Pellett, J. D., Becker, D. F., Saenger, A. K., Fuchs, J. A., and Stankovich, M. T. (2001) Role of aromatic stacking interactions in the modulation of the two-electron reduction potentials of flavin and substrate/product in Megasphaera elsdenii short-chain acyl-coenzyme A dehydrogenase, *Biochemistry 40*, 7720−7728.

17. Hauge, J. G., Crane, F. L., and Beinert, H. (1956) On the mechanism of dehydrogenation of fatty acyl derivatives of coenzyme A. III. Palmityl coa dehydrogenase, *J. Biol. Chem. 219*, 727−733.

18. Schopfer, L. M., Massey, V., Ghisla, S., and Thorpe, C. (1988) Oxidation−reduction of general acyl-CoA dehydrogenase by the butyryl-CoA/crotonyl-CoA couple. A new investigation of the rapid reaction kinetics, *Biochemistry 27*, 6599−6611.

19. Cummings, J. G., and Thorpe, C. (1994) 3-Methyleneoctanoyl-CoA and 3-methyl-*trans*-2-octenoyl-CoA: two new mechanism-based inhibitors of medium chain acyl-CoA dehydrogenase from pig kidney, *Biochemistry 41*, 788−797.

20. Corydon, T. J., Bross, P., Jensen, T. G., Corydon, M. J., Lund, T. B., Jensen, U., Kim, J.-J., Gregersen, N., and Bolund, L. A. (1998) Rapid degradation of short-chain acyl-CoA dehydrogenase variants with temperature-sensitive folding defects occurs after import into mitochondria, *J. Biol. Chem. 273*, 13065−13071.

21. Naito, E., Indo, Y., and Tanaka, K. (1990) Identification of two variant short chain acyl-coenzyme A dehydrogenase alleles, each containing a different point mutation in a patient with short chain acyl-coenzyme A dehydrogenase deficiency, *J. Clin. Invest. 85*, 1575−1582.